Dietary Curcumin Supplement Promotes Browning and Energy Expenditure in Postnatal Overfed Rats

Xiaolei Zhu
Children's Hospital of Nanjing Medical University
Susu Du
Children's Hospital of Nanjing Medical University
Qinhui Yan
Children's Hospital of Nanjing Medical University
Cuiting Min
Children's Hospital of Nanjing Medical University
Nan Zhou
Children's Hospital of Nanjing Medical University
Wei Zhou
Children's Hospital of Nanjing Medical University
Xiaonan Li (xiaonan6189@163.com)
Children's Hospital of Nanjing Medical University

Research

Keywords: Obesity, Postnatal overfeeding, Curcumin, Browning of white adipose tissue, Energy metabolism

Posted Date: August 25th, 2020

DOI: https://doi.org/10.21203/rs.3.rs-63467/v1

Abstract

Background: Early postnatal overfeeding could result in metabolic imprinting that decreases energy expenditure and induces white adipose tissue (WAT) gain throughout life. The aim of this study is to investigate the effect of curcumin (CUR) on thermogenesis and WAT browning in postnatal overfed rats.

Methods and results: Litter sizes were adjusted to three (small litters, SL) or ten (normal litters, NL) to mimic early postnatal overfeeding or normal feeding from postnatal day 3. After weaning, the SL rats were fed with a standard diet (SL) or a diet supplemented with 1% ($SL_{1\%CUR}$) or 2% ($SL_{2\%CUR}$) CUR for ten weeks. At postnatal 13 weeks, SL rats with 1% or 2% CUR supplement had lower body weight and less WAT gain, had increased lean mass ratio, and their glucose tolerance and blood lipid levels had recovered to normal when compared to SL rats that did not receive the supplement. Moreover, increased respiratory exchange ratio (RER) and heat production were consistent with the expression of uncoupling protein 1 (UCP1) and other browning-related genes in the subcutaneous adipose tissue (SAT) of the $SL_{2\%\ CUR}$ rats but not of the $SL_{1\%\ CUR}$ rats. In addition, 2% CUR dietary supplement enhanced the serum norepinephrine (NE) levels in SL rats, which was accompanied by upregulated mRNA levels of β3-adrenergic receptor (β3-AR) in SAT.

Conclusion: Dietary CUR supplement attenuates body weight gain and metabolic disorders of SL rats. The beneficial effects were probably induced by promoting browning of SAT and energy expenditure, and it was more effective in SL with 2% CUR supplement.

1. Background

Obesity is increasingly prevalent and has become a chronic metabolic disease caused by a long-term imbalance of energy intake and expenditure[1]. Numerous studies about different nutrition exposures across species have shown that an early-life obesogenic environment could lead to perturbations in the regulation of energy balance and energy-sensing pathways in later life[2], but the mechanism remains to be elucidated. Modulation of litter size is an ideal rodent model described as reducing or increasing the number of pups in a litter in order to induce neonatal over- or under-feeding, respectively[3]. Artificially small litters (SL) of three to four pups versus eight to twelve pups in control litters allow increased breast milk availability and consumption for SL pups. Milk from SL mothers is also especially enriched in triglyceride (TG) compared to control mothers[4, 5].

Our previous study indicated that postnatal overfeeding in SL rearing (3 pups) could decrease the level of body energy expenditure and this situation can persist to adulthood[6]. Therefore, on the basis of developmental plasticity, exploring the possibility of regaining energy metabolism balance and discovering its mechanism could provide potential clues for pursuing solutions for obesity and its related metabolic diseases caused by early overfeeding.

Adipose tissue is a central metabolic organ in the regulation of whole-body energy homeostasis[7]. White adipose tissue (WAT) is the primary site for storage of excess fat, and brown adipose tissue (BAT) is

responsible for non-shivering thermogenesis, in which energy is dissipated as heat[8]. As one of the principles to treat obesity is to cause an increase in energy expenditure, induction of thermogenesis in BAT is a promising method for the treatment of obesity[9, 10]. However, the amount of BAT in adults is quite small. Fortunately, brown-like adipocytes called beige adipocytes have been found in WAT. These adipocytes express uncoupling protein 1 (UCP1) to dissipate energy, similar to brown adipocytes[11, 12], in a process known as WAT browning. UCP1, a thermogenic marker, is highly expressed both in BAT and beige adipocytes. In addition, both brown and beige adipocytes express peroxisome proliferator-activated receptor γ coactivator-1α (PGC1α), a master regulator of energy metabolism[8] which is involved in mitochondrial biosynthesis. Moreover, PGC1α acts as a cofactor that will combine peroxisome proliferators-activated receptors γ (PPARγ) with positive regulatory domain containing 16 (PRDM16) to increase the expression of UCP1 in WAT[13–15]. A growing number of scientific researchers are attempting to exploit the induction of WAT browning in addition to inducing thermogenesis in BAT to address energy metabolism disorders and help individuals maintain a healthy body weight.

Curcumin (CUR) derived from turmeric (Curcuma longa Linn.) is a natural flavonoid component traditionally used as a spice and coloring in foods [16]. Many studies have given evidence of its biological effects, including anti-inflammatory, anti-cancer, anti-neurodegenerative disease and anti-cardiovascular disease[17, 18]. Recently, Wang et al. showed that a dietary CUR supplement improved insulin sensitivity and decreased body fat in mice with high-fat diet (HFD)-induced obesity [19] and obese/diabetic mice[20]. A dietary CUR supplement has been shown to relieve low-grade chronic WAT inflammation and upregulate BAT UCP1 expression in HFD mice[21]. In addition, CUR has been reported to be an anti-adipocyte dietary bioactive component largely involved in modulating the early stage of adipocyte differentiation[22]. All these findings suggest that a dietary CUR supplement might be a potential strategy to control obesity by WAT browning.

It is well known that the postnatal period is a sensitive window for WAT development. Overnutrition in early life (fetal or newborn periods) can impact adipocyte proliferation, differentiation and energy homoeostasis in adulthood [23]. CUR has the ability to prevent obesity and metabolic disorder, but its effects on postnatal overfeeding remain unknown. We hypothesized that adding a CUR supplement to the postweaning diet could promote WAT browning and energy expenditure, thereby preventing obesity and metabolic disorders in postnatal overfed rats induced by SL rearing.

2. Methods

2.1 Animals

All animal experimental and care procedures were conducted in accordance with the guidelines of the University Committee on the Use and Care of Animals and were overseen by the Unit for Laboratory Animal Medicine at Nanjing Medical University (Permit No. 1905046). Sprague-Dawley rats (Nanjing, Jiangsu, China) were maintained under standard laboratory conditions (a 12/12-h light/dark cycle, 22 ~ 24℃, 40%~60% humidity) with free access to tap water and food.

2.2 Experimental design

Artificially small litters of three to four pups (versus eight to twelve pups in normal litters) allow increased breast milk availability and induce postnatal overfeeding, which mimics over-nutrition during suckling in humans[3]. In rats, the weaning period is postnatal week 3 (W3), puberty occurs at W6-8, and adulthood is W9 and afterwards [24].

Our previous studies showed that metabolic disorders caused by postnatal overfeeding took place early at W3 and persisted to W13-16[6, 25]. Therefore, W3 and W13 were selected as two critical experimental time points to examine the effects of early nutrition on adult health conditions in our study.

The experimental protocol is shown in Fig. 1. Briefly, male pups were randomly redistributed to litter sizes of three (small litters, SL) or ten (normal litters, NL) to induce early overfeeding or normal feeding respectively from postnatal day 3[26, 27]. After weaning (W3), the NL rats were fed with a standard diet (NL group, $n = 9$), and the SL rats were fed with either a standard diet (SL group, $n = 6$) or a diet supplemented with 1% ($SL_{1\%\ CUR}$ group, $n = 9$) or 2% CUR ($SL_{2\%\ CUR}$ group, $n = 6$) until W13. CUR was purchased from Oranika Health Products (95% standardized CUR extract, Richmond, British, Canada). Body weight and food intakes were monitored weekly at a fixed time point. The specific experiments at each time point are shown in Fig. 1.

2.3 Fat mass analysis by Magnetic Resonance Imaging (MRI)

MRI was performed with a 7T Bruker BioSpec 70/20USR scanner. The rats were weighed before the MRI scanning and then anesthetized with isoflurane (5% for induction, 1–2% for maintenance) mixed with compressed air (1 liter/min) delivered through a nasal mask. Once anesthetized, the rats were placed stably in a head-holder to assure reproducible positioning inside the magnet. Respiration rate was monitored and maintained around 60–80 breaths per min throughout the experimental period. Axial sections for the analysis of fat were selected from the liver to the bladder. Two sets of multi-slice spin-echo sequence (TR = 3604.5 ms, TE = 33.0 ms) were used to acquire 35 T2-weighted anatomical axial slices per rat for W3 rats or 70 for W10 rats, with the thickness of 1.50 mm. The field of view was selected with $4.77 \times 4.50\ cm^2$ (W3 rats) or $7.03 \times 6.63\ cm^2$ (W10 rats), and matrix size was interpolated to 256 × 256, three averages per slice.

Regions of interest for each of the fat samples were manually defined in each slice of the images (Image J software, National Institutes of Health, USA), and pixel areas were measured. The fat surface area per slice was multiplied by the inter-slice distance to yield the corresponding fat volume. Total body fat volume (cm^3) was converted to mass (grams) by multiplying by $0.9196\ g/cm^3$, the assumed density of fat[28], and the percent of body fat was roughly estimated by (body fat mass/body weight) * 100%. The body weight minus body fat mass was the lean mass, and the percent of lean mass was calculated as (lean mass/body weight) * 100%.

2.4 Intraperitoneal glucose tolerance test (IPGTT)

The IPGTT was performed as described previously[29]. In brief, rats fasted overnight at W3 and W13, and a small drop of blood from the tail was placed on a glucose meter (Accu-Chek, Roche Diagnostics, Mannheim, Germany) to measure glucose levels. Next, D-Glucose (2.0 g/kg body weight) was administered intraperitoneally, and blood glucose levels were measured at 30-, 60-, 90- and 120-min intervals after the glucose injection. Then the area under the curve (AUC) was quantified.

2.5 Energy expenditure

At W13, rats were individually monitored in a custom cage. Their whole-body metabolic rate including oxygen consumption (VO_2), carbon dioxide production (VCO_2), respiratory exchange ratio (RER) and heat production were measured using an indirect calorimetry and locomotor activity monitoring system (TSE Phenomaster, TSE, Germany)[30]. To acclimate to the test chambers, rats were placed in the metabolic cages for 72 h and then monitored for an additional 24 h. The data from the final 24 h were used to calculate all parameters for which the results were reported, and the cumulative energy expenditure during the final 24 h was calculated. The rats in each chamber had free access to food and water.

2.6 Serum and tissue collection

At W3 and W13, the rats fasted overnight and were anaesthetized with chloral hydrate (300 mg/kg body weight, i.p.). Blood samples were obtained by left ventricle puncture and centrifuged at 2000 × g, 4 °C for 15 min to collect serum, then stored at -80 °C for subsequent determination of biochemical parameters. The BAT and three main types of WAT (i.e., subcutaneous adipose tissue (SAT), epididymal adipose tissue (EAT) and retroperitoneal adipose tissue (RAT)) were rapidly isolated and weighed. A portion of SAT was fixed in 4% paraformaldehyde for sectioning and staining, and the rest was rapidly frozen in liquid nitrogen and stored at -80℃ until further analysis.

2.7 Serum measurements

The content of serum aspartate aminotransferase (AST), alanine aminotransferase (ALT), total cholesterol (TC), TG, high-density lipoprotein cholesterol (HDL-C) and low-density lipoprotein cholesterol (LDL-C) were determined using an automatic biochemical analyzer (7100, Hitachi, Japan). Serum norepinephrine (NE) and insulin levels were measured using ELISA Kits (Rat Norepinephrine ELISA Kit CSB-E07022r, Rat Insulin ELISA Kit CSB-E05070r, CUSABIO, China).

2.8 Histological analysis of adipose tissue

SAT was fixed in 4% paraformaldehyde overnight at room temperature, paraffin embedded and sectioned. Tissue sections were de-waxed and rehydrated before undergoing standard hematoxylin and eosin (H&E) staining. Four arbitrary fields of view per rat were analyzed by Image J to estimate the adipocyte area.

2.9 RNA isolation and real-time quantitative polymerase chain reaction (RT-qPCR)

Total RNA was extracted from frozen SAT using TRIzol reagent (TAKARA, Japan) according to the manufacturer's instructions and quantified spectrophotometrically at OD260. The integrity of the total RNA was assessed using agarose gel electrophoresis. cDNA was prepared using 1 ug total RNA by M-MLV reverse transcriptase (TAKARA, Japan) as recommended by the manufacturer. RT-qPCR was performed on a Quant Studio 3 real-time PCR machine (Applied Biosystems, USA) using the SYBR Green master mix (Vazyme, China). Fold changes were calculated using the method of $2^{-\Delta\Delta Ct}$[31], and expression levels were normalized to the average of the housekeeping genes glyceraldehyde-3-phosphate dehydrogenase (GAPDH). The primer sequences are shown in Table 1.

Table 1
Primer sequences used for mRNA quantification by RT-qPCR

	Forward primer 5'-3'	Reverse primer 5'-3'
Ucp1	ACTGTACAGAGCTGGTGACA	TGGTAGAGAGTTGATGAATCTCGT
PGC1α	GTGGATGAAGACGGATTGCC	TTCTGAGTGCTAAGACCGCT
PRDM16	GGACAGTGACAGAGACAAAAGC	CTGTGAATAGAAGGCCGGTA
TMEM26	TTGCCATGGGCTAGAATCCG	TAAAGGCCTGTGCAGCTACC
PPARγ	ATCAGGTTTGGGCGAATG	TTTGGTCAGCGGGAAGGA
β3-AR	TGCTGTTCCTTTGCCTCCAA	TAGCTACGACGAACACTCGA
GAPDH	GGCTCTCTGCTCCTCCCTGTTCTA	CGTCCGATACGGCCAAATCCGT

2.10 Western blot analysis

Rat SAT was homogenized in ice-cold RIPA lysis buffer (50 mM Tris-HCl, pH 7.4, 0.5M NaCl, 0.25% deoxycholic acid, 1% NP-40 and 1 mM EDTA) containing a protease inhibitor cocktail. The proteins were subjected to SDS-polyacrylamide gel electrophoresis on 12% gels under reducing or non-reducing conditions and then transferred onto a polyvinylidene difluoride membrane (Bio-Rad, USA). The membranes were blocked with 5% dry non-fat milk and probed with anti-UCP1 (Abcam, USA) or anti-GAPDH (Proteintech, China) antibodies, followed by incubation with a horseradish peroxidase-conjugated secondary antibody. The reaction was detected with a chemiluminescence system (ChemiDoc XRS+, Bio-Rad, USA). The band intensity was measured by Image Lab (Bio-Rad, USA).

2.11 Statistical analyses

All results were normally distributed and presented as the mean ± standard error of the mean. Significant differences between groups at W3 were analyzed using Student's unpaired *t*-test and at W13 using one-

way analysis of variance (ANOVA) and followed by a post hoc least significant difference (LSD) *t*-test. A *p*-value < 0.05 was considered to be statistically significant.

3. Results

3.1 Bodyweight, food intake and liver enzymes

As shown in Fig. 2, the body weight gain and food intake in all groups changed with age. Body weight gain was significantly higher in SL rats than in NL at W3 and persisted to W13. The weight gains in both $SL_{1\%\ CUR}$ and $SL_{2\%\ CUR}$ rats were lower compared to SL rats after intervention for 4 weeks (Fig. 2A). There was no difference in food intake between NL and SL after W6. The rats fed CUR did not differ in food intake compared with the SL rats (Fig. 2B).

Next, we determined if the CUR supplementation had a significant effect on liver function. The SL rats showed a marked increase in their serum AST compared with the NL rats at W3, but there was no significant difference in serum ALT (Fig. 2C and D). Moreover, the levels of serum AST and ALT in SL, $SL_{1\%\ CUR}$ and $SL_{2\%\ CUR}$ rats were not different from those of the NL rats at W13 (Fig. 2C and D).

3.2 Body composition, adipose tissue mass and size

The differences of body composition between groups at W3 and W10 are shown in Fig. 3. The fat volume and body fat percentage of SL rats were higher than those of NL rats at W3 and W10. Compared to SL rats, $SL_{1\%\ CUR}$ rats had decreased fat volume and body fat percentage at W10 (Fig. 3A). The fat volume and body fat percentage in $SL_{2\%\ CUR}$ rats were significantly lower than those of SL rats and similar to those of NL rats at W10, but this was not true for the $SL_{1\%\ CUR}$ rats (Fig. 3B and C).

The lean mass in SL rats with or without CUR supplement was more than that in the NL rats at W10 and the concentration of 2% was more obvious (Fig. 3D). However, the opposite was true for lean percentage as shown in Fig. 3E.

Similarly, BAT and WAT (i.e., SAT, EAT and RAT) weight in SL rats were higher than in NL rats at W3 and W13 (Table 2). The MRI results showed that the three main types of WAT weight of $SL_{1\%\ CUR}$ and $SL_{2\%\ CUR}$ rats were lower than those of SL rats, but there was no difference of BAT weight among SL, $SL_{1\%\ CUR}$ and $SL_{2\%\ CUR}$ rats (Table 2). Furthermore, the mass ratio of BAT to WAT was lower in SL rats than in NL rats at W3 and W13, while that of both $SL_{1\%\ CUR}$ and $SL_{2\%\ CUR}$ rats was close to normal (Table 2). Histologically, the average surface area of subcutaneous white adipocyte of the SL rats was larger than that in the NL rats at W3 and W13. As expected, the average cross-sectional adipocyte area of SAT in both the $SL_{1\%\ CUR}$ and $SL_{2\%\ CUR}$ rats was much smaller than that in the SL rats (Fig. 4A and B).

Table 2
Adipose tissue weights in rats at W3 and W13

	NL	SL	$SL_{1\% CUR}$	$SL_{2\% CUR}$
W3				
BAT(g)	0.11 ± 0.01	0.20 ± 0.02[a]		
SAT(g)	0.56 ± 0.05	1.58 ± 0.04[a]		
EAT(g)	0.08 ± 0.00	0.25 ± 0.03[a]		
RAT(g)	0.08 ± 0.00	0.30 ± 0.03[a]		
BAT/WAT	0.17 ± 0.02	0.09 ± 0.01[a]		
W13				
BAT(g)	0.29 ± 0.02	0.37 ± 0.31[a]	0.32 ± 0.04	0.31 ± 0.31
SAT(g)	4.43 ± 0.37	9.39 ± 1.27[a]	5.64 ± 0.32[ab]	5.74 ± 0.50[ab]
EAT(g)	3.60 ± 0.34	7.20 ± 0.33[a]	4.56 ± 0.26[ab]	4.50 ± 0.42[b]
RAT(g)	2.54 ± 0.18	7.37 ± 0.89[a]	3.57 ± 0.31[ab]	4.77 ± 0.48[ab]
BAT/WAT	0.028 ± 0.002	0.0160 ± 0.002[a]	0.024 ± 0.003[b]	0.022 ± 0.002[b]

All values represent means ± SEM. [a]$p < 0.05$ vs. NL, [b]$p < 0.05$ vs. SL. Student's unpaired *t*-test at W3 and one-way analysis of variance (ANOVA) at W13 were performed. $n = 6–9$ in each group.

3.3 Glucose homeostasis and serum lipids

The results of IPGTT, a proxy measure of insulin sensitivity, showed that the SL rats had a greater area under the curve (AUC) for plasma glucose than the NL rats at weaning (W3) and this persisted to adulthood (W13), indicating that glucose tolerance is impaired in the SL rats. At W13, the AUC of the $SL_{1\% CUR}$ and $SL_{2\% CUR}$ rats was smaller compared with the SL rats and recovered to a normal level (Fig. 5A and B, D and E). Consistently, the serum insulin of the SL rats is higher than that of the NL rats, but the serum insulin in the $SL_{1\% CUR}$ and $SL_{2\% CUR}$ rats recovered to normal levels (Fig. 5C and F).

Moreover, serum HDL-C in the SL rats was lower than that of the NL rats at W3, and there were no significant differences in serum TC, TG, and LDL-C between the NL and SL rats (Table 3). Notably, the serum TC, TG, and LDL-C of the SL rats were all evidently higher than those of the NL rats at W13, while those of both the $SL_{1\% CUR}$ and $SL_{2\% CUR}$ rats were reduced compared with the SL rats and close to normal levels. There were no differences in the level of serum HDL-C among groups (Table 3).

Table 3
Serum lipid biochemical parameters in rats at W3 and W13

	NL	SL	$SL_{1\% CUR}$	$SL_{2\% CUR}$
W3				
TC (mg/dl)	2.14 ± 0.09	2.00 ± 0.15		
TG (mmol/L)	0.59 ± 0.13	0.64 ± 0.13		
HDL-C (mmol/L)	0.59 ± 0.01	0.46 ± 0.05[a]		
LDL-C (mmol/L)	0.52 ± 0.04	0.55 ± 0.30		
W13				
TC (mg/dl)	1.59 ± 0.07	1.85 ± 0.07[a]	1.54 ± 0.08[b]	1.47 ± 0.06[b]
TG (mmol/L)	0.63 ± 0.05	1.23 ± 0.13[a]	0.66 ± 0.09[b]	0.57 ± 0.04[b]
HDL-C (mmol/L)	0.38 ± 0.01	0.36 ± 0.03	0.34 ± 0.03	0.37 ± 0.02
LDL-C (mmol/L)	0.41 ± 0.03	0.61 ± 0.03[a]	0.44 ± 0.04[b]	0.47 ± 0.02[b]

All values represent means ± SEM. [a]$p < 0.05$ vs. NL, [b]$p < 0.05$ vs. SL. Student's unpaired *t*-test at W3 and ANOVA at W13 were performed. $n = 6–9$ in each group.

3.4 Energy expenditure

At W13, the O_2 consumption (Fig. 6A and B), CO_2 production (Fig. 6C and D), respiratory exchange ratio (Fig. 6E and F), and heat production (Fig. 6G and H) of the SL rats were all lower than those of the NL rats. Compared to the SL rats, the level of O_2 consumption, CO_2 production, respiratory exchange ratio, and heat production were improved significantly in the $SL_{2\% CUR}$ rats but not in the $SL_{1\% CUR}$ rats.

3.5 Expression of browning-regulating and thermogenic genes in SAT

We measured several genes in SAT that are involved in the transformation of white into beige adipose tissue and thermogenesis to evaluate the effect of CUR on the acquisition of beige adipose tissue characteristics by white adipocytes. Compared to the NL rats, the expression of UCP1 in the SL rats was inhibited at W3 and W13 but was significantly upregulated by dietary CUR supplementation in the SL rats. This trend became more obvious in the 2% CUR supplement rats at W13 (Fig. 7A-C). Subsequently, the mRNA levels of PGC1α in SAT were consistent with that of UCP1 (Fig. 7D).

In addition, the mRNA level of PRDM16 was decreased in the SL rats, and the expression levels of TMEM26 and PPARγ were not significantly different between the NL and SL rats at W3 (Fig. 7E). However,

the mRNA levels of PRDM16, TMEM26 and PPARγ were suppressed in the SL rats compared to the NL rats at W13 and enhanced in the SAT of the SL rats treated with dietary CUR, as expected. Likewise, the mRNA levels were enhanced in the $SL_{2\%\ CUR}$ rats (Fig. 7F).

3.6 Serum NE levels and β3-ARgene expression in SAT

The UCP1-mediated thermogenic response is regulated primarily by the sympathetic nervous system through the binding of NE to the β3-AR. We examined whether CUR affects NE release and the expression of its receptor. As shown in Fig. 8A, the levels of serum NE were deceased in the SL rats compared to those in the NL rats at W3 and W13. Moreover, the serum NE reached a normal level only in the $SL_{2\%\ CUR}$ rats. The pattern of β3-AR mRNA expression in SAT among groups was similar to their serum NE (Fig. 8B).

4. Discussion

Numerous studies have demonstrated that the postnatal nutritional environment during the suckling period could affect body weight and energy homeostasis into adulthood[32, 33]. In the present study, the rat model of postnatal overfeeding induced by SL rearing led to several metabolic alterations such as higher body weight and WAT mass, increased serum lipids and insulin resistance at weaning and adulthood. These findings were in accordance with previous studies[6, 34].

Rats fed a post-weaning diet supplemented with CUR exhibited lower body weight, less fat mass, higher energy expenditure and improved glucose and lipid metabolism in adulthood compared to a standard diet in SL-reared rats. Furthermore, UCP1-positive brown fat-like cells emerged in the SAT of these rats after the CUR intervention. These data suggest that a dietary CUR supplement could stimulate the development of WAT browning and might be a strategy to increase energy expenditure for preventing obesity induced by postnatal overfeeding.

CUR's capacity as an anti-obesity nutraceutical that increases weight loss and lowers fat mass has been verified previously in models of obesity at adulthood[20, 35]. The present study is the first to show this effect in overfed rats in the SL-rearing model. Recent studies have identified several windows of opportunity from preconception to childhood during which interventions could have long-lasting effects that could halt the transgenerational cycle of obesity and type 2 diabetes[36]. In this study, we found that dietary CUR supplementation after weaning ($SL_{1\%\ CUR}$ and $SL_{2\%\ CUR}$ rats) was effective to reduce body weight, adipose tissue mass, and adipocyte volume in rats. Many metabolic diseases are increasing in parallel with the prevalence of obesity and overweight in youth, including type 2 diabetes, insulin resistance and hyperlipidemia[37, 38]. Interestingly, this study initially found that dietary CUR supplementation was also useful in improving glucose intolerance and hyperlipidemia induced by postnatal overfeeding.

The balance of energy intake and energy expenditure is the basis for maintaining a healthy body weight. The rationales of treatments for weight loss usually include reducing total energy uptake and increasing

energy expenditure[39]. In the present study, dietary administration of CUR (1% or 2% diet) increased energy expenditure but did not affect food intake in SL rats, which suggests that CUR could enhance energy metabolism rather than inhibit energy intake. Evidence from in vitro and in vivo studies has shown that CUR can increase the basal metabolic rate, thereby contributing to increased energy expenditure[40]. Unsurprisingly, we observed an increase in the energy expenditure of SL rats fed a diet containing 2% CUR.

Adipose tissue is a critical regulator of systemic energy homeostasis by acting as a caloric reservoir[7]. Induction of WAT browning could increase energy consumption and help to alleviate metabolic disorders[9–11]. Upregulation of UCP1 expression is closely related to increased adaptive thermogenic and energy expenditure and is widely used as a marker during BAT activity and WAT browning[41]. In rodents, WAT depots have different propensities to form beige adipocytes[42]. Induction of WAT browning occurs easily in subcutaneous depots compared with visceral mesenteric or epididymal depots[43, 44]. In this study, we mainly observed the browning feature of CUR in SAT and found that 2% dietary CUR supplement could increase both UCP1 mRNA and protein expression levels in the SAT of SL rats. The transcription of UCP1 requires coactivators, including PGC1α, PRDM16 and PPARγ[<link rid="bib9">9</link>], which returned to normal levels in $SL_{2\%\ CUR}$ rats. Puigserver et al. have shown that ectopic expression of PGC1α in WAT depots is required to commit the cells to thermogenesis[45].

PGC1α is also a regulator of mitochondrial biogenesis, which is another characteristic manifestation of browning[46]. Moreover, transmembrane protein 26 (TMEM26)[8], a specific beige-selective gene that can distinguish beige adipocytes from brown or white adipocytes in adipose tissues, was upregulated in the SAT of SL rats with a diet containing 2% CUR. Taken together, these findings indicate that CUR may act as a thermogenic activator to promote the browning of SAT. This function could explain, at least in part, the positive effects of the dietary CUR intervention on metabolic disorders in obese rats induced by postnatal overfeeding.

Furthermore, we observed the serum NE and β3-ARmRNA expression levels in the SAT of rats. The release of NE from the adrenal medulla and sympathetic terminals in WAT is mandatory for the immediate activation of existing beige adipocytes and the differentiation of beige adipocytes from their precursors[47]. NE acts on the β3-AR expressed in brown/beige adipocytes and then activates c-AMP pathway-dependent mitochondrial UCP1, which is the major mediator of adaptive thermogenesis in brown and beige adipose tissue[8]. Many factors activate the β3-AR signaling pathway in WAT; the most effective is chronic cold exposure, which could induce the browning process[48].

In this study, we found that the SL rats experienced a decrease in serum NE and β3-AR mRNA expression levels in their SAT at both W3 and W13, but this could be reversed by feeding them a 2% CUR dietary supplement post-weaning. In vitro, we found that the expression of browning marker genes was significantly increased following treatment of CUR in preadipocytes, and the increase was suppressed by β3-AR antagonist[49]. Taken together, our findings support that CUR-induced SAT browning may be associated with sympathetic stimulation through the norepinephrine-β3-AR pathway.

The effects of functional foods are ordinarily influenced by the dose administered[50]. Generally, orally ingested CUR is metabolized in the liver and small intestine, and liver enzymes (AST and ALT) are usually used to detect oral toxicity[51]. There was no significant difference in the serum AST and ALT levels in the $SL_{1\%\ CUR}$ or $SL_{2\%CUR}$ rats compared to the NL rats, which suggests that neither dose of CUR used in the present study resulted in liver injury.

In previous studies, the major intervention for CUR in obese animal models was oral administration, including gavage and dietary supplementation. The concentrations used in the latter range widely, from 0.1–3%. In this study, we provided the SL rats with two different doses of CUR (95% standardized CUR extract) to understand the effects of dose difference. The doses set in the current study are 1% and 2%, referring to the concentration of dietary CUR (95% standardized CUR extract) used in previous studies on obese mice models induced by high-fat diet and Western diet, which were 1% and 3%, respectively.

In the present study, the changes of body weight, serum chemical parameters, adipocyte surface area, and energy expenditure as well as expressions of browning-related genes in the $SL_{2\%CUR}$ rats were slightly better than those of the $SL_{1\%CUR}$ rats, but there were no statistical differences in these obesity parameters and browning genes between the $SL_{1\%\ CUR}$ and $SL_{2\%CUR}$ rats. Therefore, dietary 2% CUR supplementation seemed to be an efficient dose for an anti-obesity effect, but we cannot exclude that the effects may be enhanced by a higher dose of CUR.

5. Conclusions

A post-weaning diet supplemented with CUR significantly improved obesity and metabolic disorders in overfed rats induced by SL rearing, probably through triggering energy metabolism remodeling and upregulating the browning-regulated gene expression in SAT. Importantly, CUR stimulated the browning program possibly regulated by NE/β3-AR. Further studies investigating other thermogenic organs and their molecular pathways are still required. Based on these findings, we concluded that CUR as a natural and edible plant could be a potential new strategy to combat postnatal overfeeding-induced obesity and related disorders.

Abbreviations

β3-AR: β3-adrenergic receptor

ALT: Alanine aminotransferase

ANOVA: Analysis of variance

AST: Aspartate aminotransferase

AUC: Area under the curve

BAT: Brown adipose tissue

CUR: Curcumin

EAT: Epididymal adipose tissue

GAPDH: Glyceraldehyde-3-phosphate dehydrogenase

HDL-C: High-density lipoprotein cholesterol

HFD: High fat diet

IPGTT: Intraperitoneal glucose tolerance test

LDL-C: Low-density lipoprotein cholesterol

LSD: Least significant difference

NE: norepinephrine

NL: Normal litters

PGC1a: Peroxisome proliferator-activated receptor γ coactivator-1a

PPARg: Peroxisome proliferators-activated receptorsg

PRDM16: Positive regulatory domain containing 16

RAT: Retroperitoneal adipose tissue

RER: Respiratory exchange ratio

SAT: Subcutaneous adipose tissue

SL: Small litters

TC: Total cholesterol

TG: Triglyceride

TMEM26: Transmembrane protein 26

UCP1: Uncoupling protein 1

VCO2: Carbon dioxide production

VO2: Oxygen consumption

WAT: white adipose tissue

W3: Postnatal week 3

W10: Postnatal week 10

W13: Postnatal week 13

Declarations

Ethics approval and consent to participate

All animal studies were performed following the guidelines established by the University Committee on the Use and Care of Animals and were overseen by the Unit for Laboratory Animal Medicine at Nanjing Medical University (IACUC: 1905046).

Consent for publication

Not applicable

Availability of data and materials

Data are all contained within the article.

Competing interests

The authors declare that there is no conflict of interest that could be perceived as prejudicing the impartiality of the research reported.

Funding

This work was supported by the National Natural Science Foundation of China (81773421), Jiangsu Province Social Development Research (BE 2015607) and Innovation Team of Jiangsu Health (CXTDA 2017035).

Authors' contributions

XZ and XL designed the study. XZ, SD and QY performed the experiments. XZ analyzed data. XZ and XL wrote the paper, and CM, NZ and WZ reviewed the manuscript. All authors had final approval of the submitted and published versions.

Acknowledgments

We thank the Department of Experimental Animals of Nanjing Medical University for their technical assistance.

References

1. Chen L-H, Chen Y-H, Cheng K-C, Chien T-Y, Chan C-H, Tsao S-P, Huang H-Y: **Antiobesity effect of Lactobacillus reuteri 263 associated with energy metabolism remodeling of white adipose tissue in high-energy-diet-fed rats**. *J Nutr Biochem* 2018, **54**:87-94.
2. Reynolds CM, Segovia SA, Vickers MH: **Experimental Models of Maternal Obesity and Neuroendocrine Programming of Metabolic Disorders in Offspring**. *Front Endocrinol (Lausanne)* 2017, **8**:245-245.
3. Marousez L, Lesage J, Eberlé D: **Epigenetics: Linking Early Postnatal Nutrition to Obesity Programming?** *Nutrients* 2019, **11**(12):E2966.
4. Šefčíková Z, Bujňáková D, Raček Ľ, Kmet V, Mozeš Š: **Developmental changes in gut microbiota and enzyme activity predict obesity risk in rats arising from reduced nests**. *Physiol Res* 2011, **60**(2):337-346.
5. Xavier JLP, Scomparin DX, Pontes CC, Ribeiro PR, Cordeiro MM, Marcondes JA, Mendonça FO, Silva MTd, Oliveira FBd, Franco GCN *et al*: **Litter Size Reduction Induces Metabolic and Histological Adjustments in Dams throughout Lactation with Early Effects on Offspring**. *An Acad Bras Cienc* 2019, **91**(1):e20170971-e20170971.
6. Dai Y, Zhou N, Yang F, Zhou S, Sha L, Wang J, Li X: **Effects of postnatal overfeeding and fish oil diet on energy expenditure in rats**. *Pediatr Res* 2018, **83**(1-1):156-163.
7. Choe SS, Huh JY, Hwang IJ, Kim JI, Kim JB: **Adipose Tissue Remodeling: Its Role in Energy Metabolism and Metabolic Disorders**. *Front Endocrinol (Lausanne)* 2016, **7**:30-30.
8. Nedergaard J, Cannon B: **The browning of white adipose tissue: some burning issues**. *Cell Metab* 2014, **20**(3):396-407.
9. Vargas-Castillo A, Fuentes-Romero R, Rodriguez-Lopez LA, Torres N, Tovar AR: **Understanding the Biology of Thermogenic Fat: Is Browning A New Approach to the Treatment of Obesity?** *Arch Med Res* 2017, **48**(5):401-413.
10. Sidossis L, Kajimura S: **Brown and beige fat in humans: thermogenic adipocytes that control energy and glucose homeostasis**. *J Clin Invest* 2015, **125**(2):478-486.
11. Lizcano F, Vargas D: **Biology of Beige Adipocyte and Possible Therapy for Type 2 Diabetes and Obesity**. *Int J Endocrinol* 2016, **2016**:9542061.
12. Garcia RA, Roemmich JN, Claycombe KJ: **Evaluation of markers of beige adipocytes in white adipose tissue of the mouse**. *Nutr Metab (Lond)* 2016, **13**:24-24.
13. Hondares E, Rosell M, Díaz-Delfín J, Olmos Y, Monsalve M, Iglesias R, Villarroya F, Giralt M: **Peroxisome proliferator-activated receptor α (PPARα) induces PPARγ coactivator 1α (PGC-1α) gene expression and contributes to thermogenic activation of brown fat: involvement of PRDM16**. *J Biol Chem* 2011, **286**(50):43112-43122.
14. Nedergaard J, Petrovic N, Lindgren EM, Jacobsson A, Cannon B: **PPARgamma in the control of brown adipocyte differentiation**. *Biochim Biophys Acta* 2005, **1740**(2):293-304.

15. Liang H, Ward WF: **PGC-1alpha: a key regulator of energy metabolism**. *Adv Physiol Educ* 2006, **30**(4):145-151.
16. Tsuda T: **Curcumin as a functional food-derived factor: degradation products, metabolites, bioactivity, and future perspectives**. *Food Funct* 2018, **9**(2):705-714.
17. Kumar G, Mittal S, Sak K, Tuli HS: **Molecular mechanisms underlying chemopreventive potential of curcumin: Current challenges and future perspectives**. *Life Sci* 2016, **148**:313-328.
18. Kunnumakkara AB, Bordoloi D, Padmavathi G, Monisha J, Roy NK, Prasad S, Aggarwal BB: **Curcumin, the golden nutraceutical: multitargeting for multiple chronic diseases**. *Br J Pharmacol* 2017, **174**(11):1325-1348.
19. Wang S, Wang X, Ye Z, Xu C, Zhang M, Ruan B, Wei M, Jiang Y, Zhang Y, Wang L *et al*: **Curcumin promotes browning of white adipose tissue in a norepinephrine-dependent way**. *Biochem Biophys Res Commun* 2015, **466**(2):247-253.
20. Weisberg SP, Leibel R, Tortoriello DV: **Dietary curcumin significantly improves obesity-associated inflammation and diabetes in mouse models of diabesity**. *Endocrinology* 2008, **149**(7):3549-3558.
21. Song Z, Revelo X, Shao W, Tian L, Zeng K, Lei H, Sun H-S, Woo M, Winer D, Jin T: **Dietary Curcumin Intervention Targets Mouse White Adipose Tissue Inflammation and Brown Adipose Tissue UCP1 Expression**. *Obesity (Silver Spring)* 2018, **26**(3):547-558.
22. Kim CY, Le TT, Chen C, Cheng J-X, Kim K-H: **Curcumin inhibits adipocyte differentiation through modulation of mitotic clonal expansion**. *J Nutr Biochem* 2011, **22**(10):910-920.
23. Mostyn A, Symonds ME: **Early programming of adipose tissue function: a large-animal perspective**. *Proc Nutr Soc* 2009, **68**(4):393-400.
24. Tirelli E, Laviola G, Adriani W: **Ontogenesis of behavioral sensitization and conditioned place preference induced by psychostimulants in laboratory rodents**. *Neurosci Biobehav Rev* 2003, **27**(1-2):163-178.
25. Ji C, Dai Y, Jiang W, Liu J, Hou M, Wang J, Burén J, Li X: **Postnatal overfeeding promotes early onset and exaggeration of high-fat diet-induced nonalcoholic fatty liver disease through disordered hepatic lipid metabolism in rats**. *J Nutr Biochem* 2014, **25**(11):1108-1116.
26. McCance RA: **Food, growth, and time**. *Lancet (London, England)* 1962, **2**(7258):671-676.
27. Velkoska E, Cole TJ, Dean RG, Burrell LM, Morris MJ: **Early undernutrition leads to long-lasting reductions in body weight and adiposity whereas increased intake increases cardiac fibrosis in male rats**. *J Nutr* 2008, **138**(9):1622-1627.
28. Tang H, Vasselli JR, Wu EX, Boozer CN, Gallagher D: **High-resolution magnetic resonance imaging tracks changes in organ and tissue mass in obese and aging rats**. *Am J Physiol Regul Integr Comp Physiol* 2002, **282**(3):R890-R899.
29. Chen H, Simar D, Lambert K, Mercier J, Morris MJ: **Maternal and postnatal overnutrition differentially impact appetite regulators and fuel metabolism**. *Endocrinology* 2008, **149**(11):5348-5356.

30. Czyzyk TA, Nogueiras R, Lockwood JF, McKinzie JH, Coskun T, Pintar JE, Hammond C, Tschöp MH, Statnick MA: **kappa-Opioid receptors control the metabolic response to a high-energy diet in mice**. *FASEB J* 2010, **24**(4):1151-1159.
31. Schmittgen TD, Livak KJ: **Analyzing real-time PCR data by the comparative C(T) method**. *Nat Protoc* 2008, **3**(6):1101-1108.
32. Ojha S, Saroha V, Symonds ME, Budge H: **Excess nutrient supply in early life and its later metabolic consequences**. *Clin Exp Pharmacol Physiol* 2013, **40**(11):817-823.
33. Symonds ME, Sebert SP, Hyatt MA, Budge H: **Nutritional programming of the metabolic syndrome**. *Nat Rev Endocrinol* 2009, **5**(11):604-610.
34. Hou M, Liu Y, Zhu L, Sun B, Guo M, Burén J, Li X: **Neonatal overfeeding induced by small litter rearing causes altered glucocorticoid metabolism in rats**. *PLoS One* 2011, **6**(11):e25726.
35. Ejaz A, Wu D, Kwan P, Meydani M: **Curcumin inhibits adipogenesis in 3T3-L1 adipocytes and angiogenesis and obesity in C57/BL mice**. *J Nutr* 2009, **139**(5):919-925.
36. Gingras V, Hivert MF, Oken E: **Early-Life Exposures and Risk of Diabetes Mellitus and Obesity**. *Curr Diab Rep* 2018, **18**(10):89.
37. Bullock A, Sheff K: **Incidence Trends of Type 1 and Type 2 Diabetes among Youths, 2002-2012**. *N Engl J Med* 2017, **377**(3):301.
38. Williams DE, Cadwell BL, Cheng YJ, Cowie CC, Gregg EW, Geiss LS, Engelgau MM, Narayan KM, Imperatore G: **Prevalence of impaired fasting glucose and its relationship with cardiovascular disease risk factors in US adolescents, 1999-2000**. *Pediatrics* 2005, **116**(5):1122-1126.
39. Singh R, Braga M, Pervin S: **Regulation of brown adipocyte metabolism by myostatin/follistatin signaling**. *Front Cell Dev Biol* 2014, **2**:60.
40. Alappat L, Awad AB: **Curcumin and obesity: evidence and mechanisms**. *Nutr Rev* 2010, **68**(12):729-738.
41. Jeremic N, Chaturvedi P, Tyagi SC: **Browning of White Fat: Novel Insight Into Factors, Mechanisms, and Therapeutics**. *J Cell Physiol* 2017, **232**(1):61-68.
42. Waldén TB, Hansen IR, Timmons JA, Cannon B, Nedergaard J: **Recruited vs. nonrecruited molecular signatures of brown, "brite," and white adipose tissues**. *Am J Physiol Endocrinol Metab* 2012, **302**(1):E19-31.
43. Cohen P, Levy JD, Zhang Y, Frontini A, Kolodin DP, Svensson KJ, Lo JC, Zeng X, Ye L, Khandekar MJ *et al*: **Ablation of PRDM16 and beige adipose causes metabolic dysfunction and a subcutaneous to visceral fat switch**. *Cell* 2014, **156**(1-2):304-316.
44. Merlin J, Evans BA, Dehvari N, Sato M, Bengtsson T, Hutchinson DS: **Could burning fat start with a brite spark? Pharmacological and nutritional ways to promote thermogenesis**. *Mol Nutr Food Res* 2016, **60**(1):18-42.
45. Puigserver P, Wu Z, Park CW, Graves R, Wright M, Spiegelman BM: **A cold-inducible coactivator of nuclear receptors linked to adaptive thermogenesis**. *Cell* 1998, **92**(6):829-839.

46. Lin J, Wu PH, Tarr PT, Lindenberg KS, St-Pierre J, Zhang CY, Mootha VK, Jäger S, Vianna CR, Reznick RM *et al*: **Defects in adaptive energy metabolism with CNS-linked hyperactivity in PGC-1alpha null mice**. *Cell* 2004, **119**(1):121-135.
47. Bartelt A, Heeren J: **Adipose tissue browning and metabolic health**. *Nat Rev Endocrinol* 2014, **10**(1):24-36.
48. Montanari T, Pošćić N, Colitti M: **Factors involved in white-to-brown adipose tissue conversion and in thermogenesis: a review**. *Obes Rev* 2017, **18**(5):495-513.
49. Zhu X, Du S, Yan Q, Zhou W, Li X: **[EFFECT AND MECHANISM OF CURCUMIN PROMOTING THE BROWNING OF MOUSE SUBCUTANEOUS PRESDIPOCYTES]**. *Journal of Nanjing Medical University (Natural Science)* 2020, **40**(6):796-802.(in Chinese).
50. Granado-Lorencio F, Hernández-Alvarez E: **Functional Foods and Health Effects: A Nutritional Biochemistry Perspective**. *Curr Med Chem* 2016, **23**(26):2929-2957.
51. Esatbeyoglu T, Huebbe P, Ernst IM, Chin D, Wagner AE, Rimbach G: **Curcumin--from molecule to biological function**. *Angew Chem Int Ed Engl* 2012, **51**(22):5308-5332.

Figures

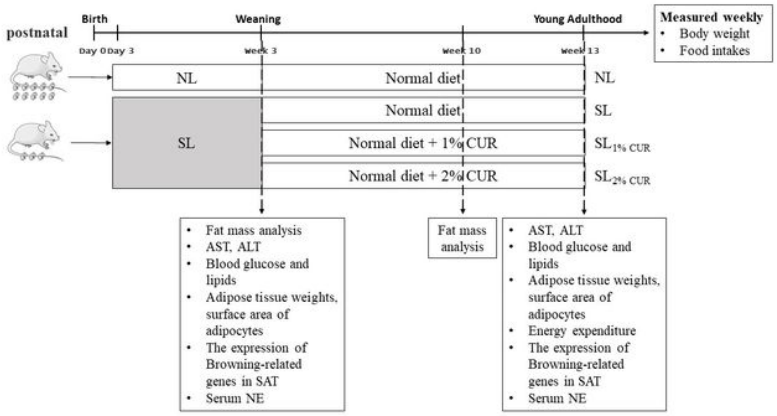

Fig.1

Figure 1

Schematic overview of the experimental design.

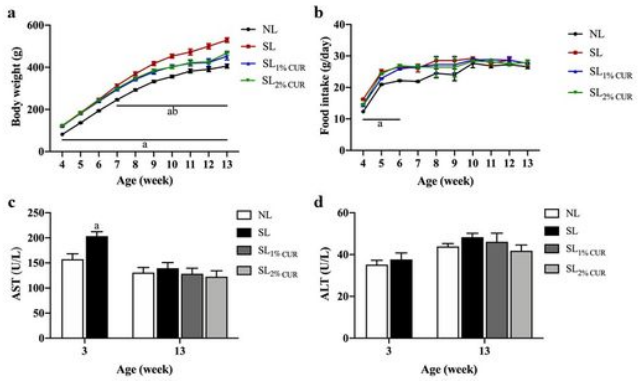

Fig.2

Figure 2

Body weight (a) and food intake in rats (b) from W4 to W13. Serum levels of aspartate aminotransferase (AST) (c) and alanine aminotransferase (ALT) (d) in rats at W3 and W13. All values represent means ± SEM. ap < 0.05 vs. NL, bp < 0.05 vs. SL. Body weight and food intake were analyzed by one-way analysis of variance (ANOVA), AST and ALT levels were analyzed by Student's unpaired t-test at W3 and one-way analysis of variance (ANOVA) at W13. n=6-9 in each group.

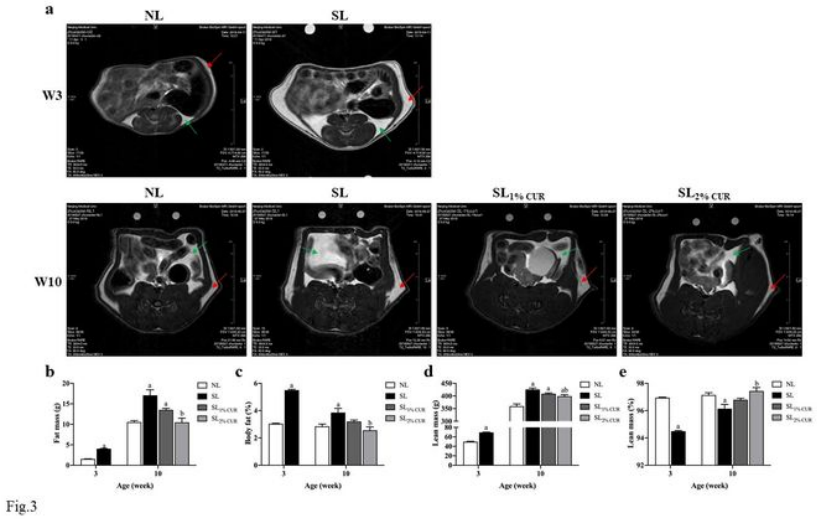

Fig.3

Figure 3

MRI analysis of body fat in rats at W3 and W10 (red arrow pointing to subcutaneous adipose tissue and green arrow pointing to visceral adipose tissue) (a) and followed by calculating fat mass (b), body fat percentage (c), lean mass (d) and lean percentage (e).All values represent means ± SEM. ap < 0.05 vs. NL, bp < 0.05 vs. SL. Statistical analysis was performed using Student's unpaired t-test at W3 and ANOVA at W10. n=3-4 in each group.

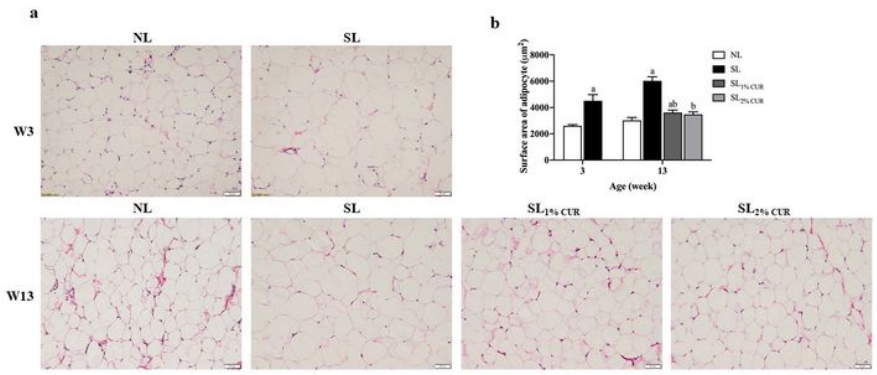

Fig.4

Figure 4

Hematoxylin and eosin (H&E) staining in sections of subcutaneous adipose tissue in rats (200×) (a) and determine the surface area of adipocyte (b) at W3 and W13. All values represent means ± SEM. ap < 0.05 vs. NL, bp < 0.05 vs. SL. Statistical analysis was performed using Student's unpaired t-test at W3 and ANOVA at W13. n=6-9 in each group.

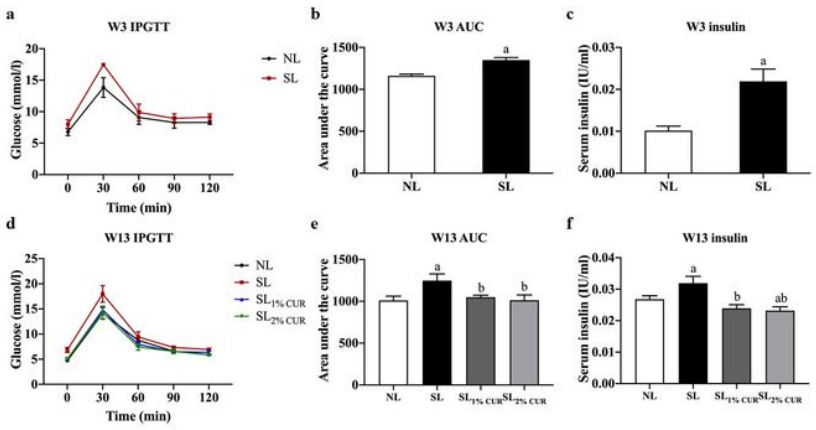

Fig.5

Figure 5

Intraperitoneal glucose tolerance test (IPGTT), area under the curve (AUC) and serum levels of insulin in rats at W3 (a-c) and W13 (d-f). All values represent means ± SEM. ap < 0.05 vs. NL, bp < 0.05 vs. SL. Statistical analysis was performed using Student's unpaired t-test at W3 and ANOVA at W13. n=6-9 in each group.

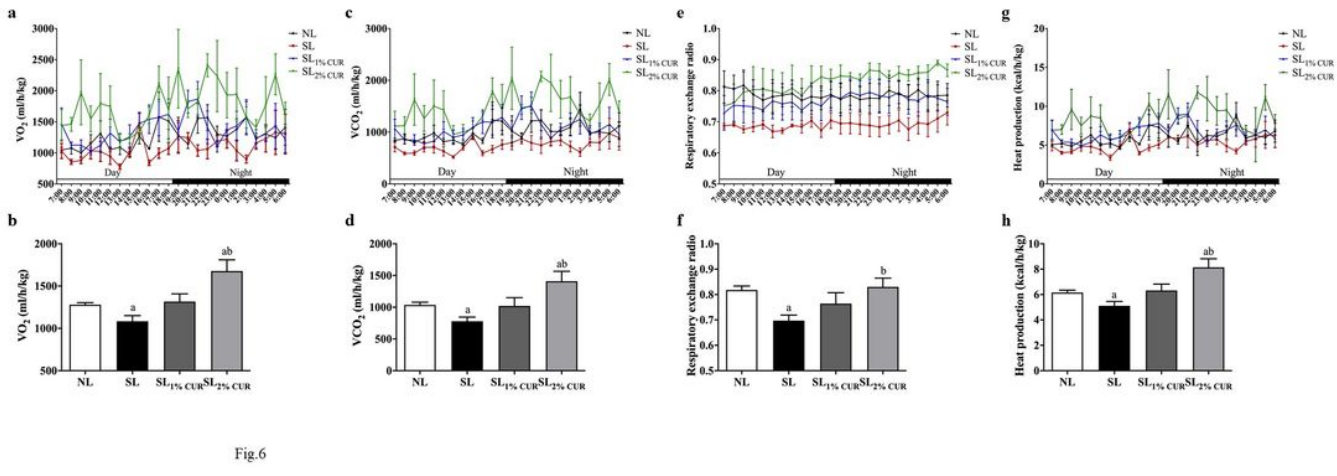

Fig.6

Figure 6

The whole-body metabolic rate including oxygen consumption (a and b), carbon dioxide production (c and d), respiratory exchange radio (e and f) and heat production (g and h) in rats at W13. All values represent means ± SEM. ap < 0.05 vs. NL, bp < 0.05 vs. SL. ANOVA was performed. n=4 in each group.

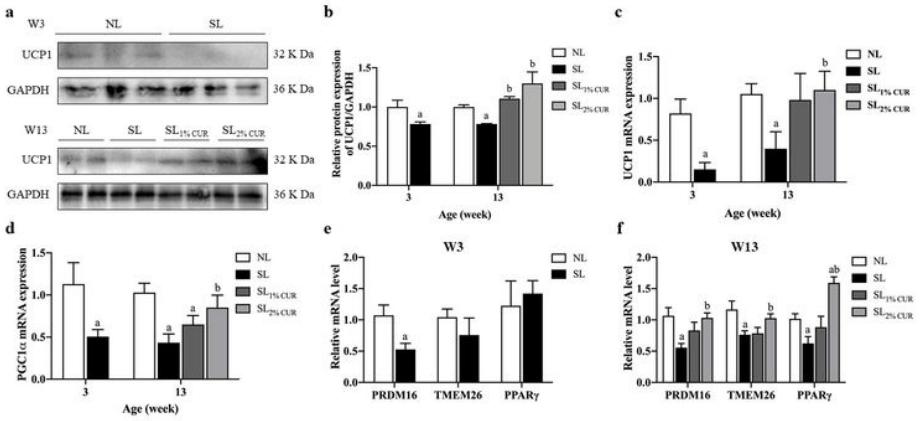

Fig. 7

Figure 7

Protein expression of UCP1 (a and b), mRNA expression of UCP1 (c) and PGC1α(d) of subcutaneous adipose tissue in rats at W3 and W13. mRNA expression of PRDM16, TMEM26 and PPARγ of subcutaneous adipose tissue in rats at W 3 (e) and W 13 (f). All values represent means ± SEM. ap < 0.05 vs. NL, bp < 0.05 vs. SL. Statistical analysis was performed using Student's unpaired t-test at W 3 and ANOVA at W13. n=6-9 in each group.

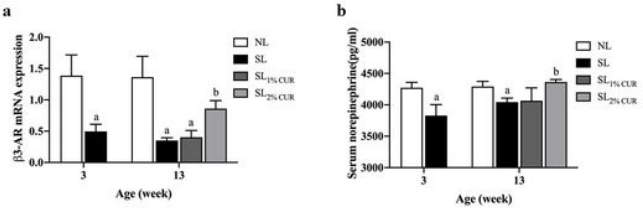

Fig. 8

Figure 8

Serum levels of norepinephrine (a) and mRNA expression of β3-AR of subcutaneous adipose tissue (b) in rats at W3 and W13. All values represent means ± SEM. ap < 0.05 vs. NL, bp < 0.05 vs. SL. Statistical analysis was performed using Student's unpaired t-test at W 3 and ANOVA at W13. n=6-9 in each group.